Supporting Information

Crystal Size Dependent Photogenerated Charge Separation on Octahedral Bismuth Vanadate Photocatalyst

Yuting Deng[a,b], Qian Li[a,b], Pengpeng Wang[a], Fengke Sun[b,c], Can Li[a] and Rengui Li*[a]

[a] State Key Laboratory of Catalysis, Dalian National Laboratory for Clean Energy, *i*ChEM (Collaborative Innovation Center of Chemistry for Energy Materials), Dalian Institute of Chemical Physics, Chinese Academy of Sciences, Dalian 116023, China

[b] Center of Materials Science and Optoelectronics Engineering, University of Chinese Academy of Sciences, Beijing 100049, China

[c] State Key Laboratory of Molecular Reaction Dynamics and the Dynamic Research Center for Energy and Environmental Materials, Dalian Institute of Chemical Physics, Chinese Academy of Sciences, Dalian 116023, China

* E-mail: rgli@dicp.ac.cn

1. Experimental section

1.1 Materials

Bismuth nitrate pentahydrate ($Bi(NO_3)_3\cdot 5H_2O$), ammonium metavanadate (NH_4VO_3), sodium dodecyl benzene sulphonate (SDBS), methanol and ferric nitrate nonahydrate ($Fe(NO_3)_3\cdot 9H_2O$) were all purchased from Sinopharm Chemical Reagent Co., Ltd. All of the reagents were directly used without further purification. Solutions were prepared using high purity water (Millipore Milli-Q purification system, resistivity > 18 MΩ·cm).

1.2 The calculation of apparent quantum efficiency (AQE)

The AQE was calculated using the following equation:

$$AQE = \frac{Number\ of\ reacted\ electrons}{Number\ of\ incident\ photons} \times 100\% \tag{S1}$$

Herein, the number of reacted electrons is obtained by the maximum photocatalytic activity under the optimized photocatalyst mass.

Generally, a photocatalytic water oxidation reaction takes place in a cascade of elementary steps, including charge carrier generation, separation and migration, and then surface catalytic reaction. The overall efficiency of solar energy conversion is directly determined by the multiplication of the efficiencies of three major processes.

$$\eta = \eta_{LH} \times \eta_{sep} \times \eta_{CU} \tag{S2}$$

(η_{LH}, efficiency of light harvesting; η_{sep}, efficiency of charge separation; η_{CU}, efficiency of charge utilization).

When a photocatalytic reaction is carried out in an aqueous solution including Fe^{3+} and methanol, Fe^{3+} and methanol would serve as electron scavengers and electron donors and rapidly consume the photogenerated charges, thus inhibiting the recombination of electrons and holes on the $BiVO_4$ surface. Since the reaction rates of both the methanol oxidation and Fe^{3+} reduction are fast enough, the effect of surface reaction kinetics is minimized. Photocatalyst mass is optimized in order that almost all the incident photons can be absorbed. Therefore, considering that η_{LH} and η_{CU} are both close to one, the obtained apparent quantum efficiency could be well approximate to the charge separation efficiency.

1.3 The measurements of the reaction rate of Fe^{3+} reduction

The measurements of charge separation efficiencies were conducted simultaneously using Fe^{3+} ions as electron acceptors and methanol as hole acceptors. The photocatalysts were dispersed in the mixture solution (100 mL) of $Fe(NO_3)_3$ aqueous solution (5.0 mM) and CH_3OH (20 vol%). The reaction rate of Fe^{3+} reduction to Fe^{2+} was determined via a phenanthroline method by UV-vis absorption.[1] The solution after reaction was diluted five times so that the concentration of Fe^{2+} is less than 1.0 mM. Then 1.0 mL diluted solution was mixed with 4.0 mL NaAc-HAc buffer solution (0.2 M, pH = 4.0) and 3.0 mL 0.1 wt% 1,10-phenanthroline solution (50 vol% ethanol solution). Then the UV-visible absorption spectrum was measured. According to the calibration equation (Equation S3), the concentration of Fe^{2+} could be obtained based on the absorbance at 510 nm, as shown in Fig. S4-S7:

$$C = 0.709 \times A + 0.007 \tag{S3}$$

where C is the concentration of Fe^{2+} in the diluted solution, A is the absorbance at 510 nm.

2. Figures

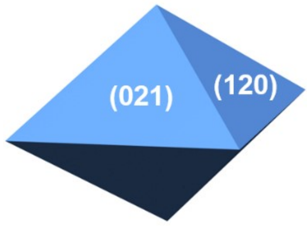

Fig. S1 Schematic illustration of $BiVO_4$ crystal exposed with {120} and {021} facets.

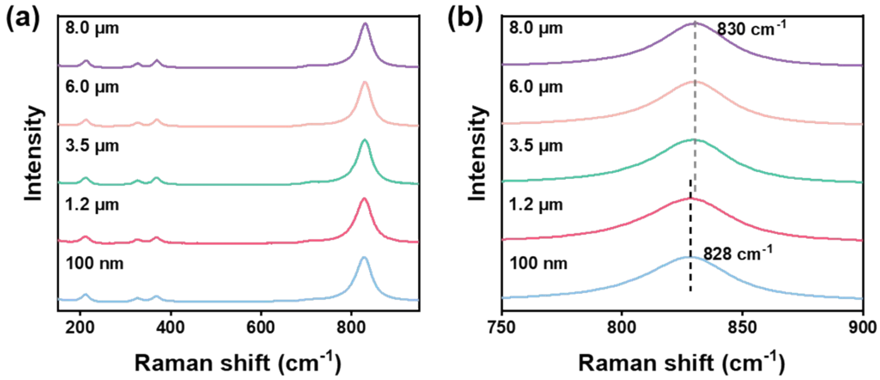

Fig. S2 Raman spectra for octahedral $BiVO_4$ crystals with different sizes.

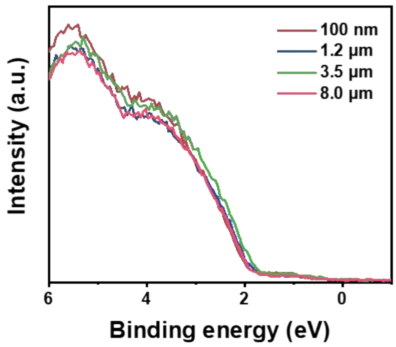

Fig. S3 XPS valance band spectra of octahedral $BiVO_4$ crystals with different sizes.

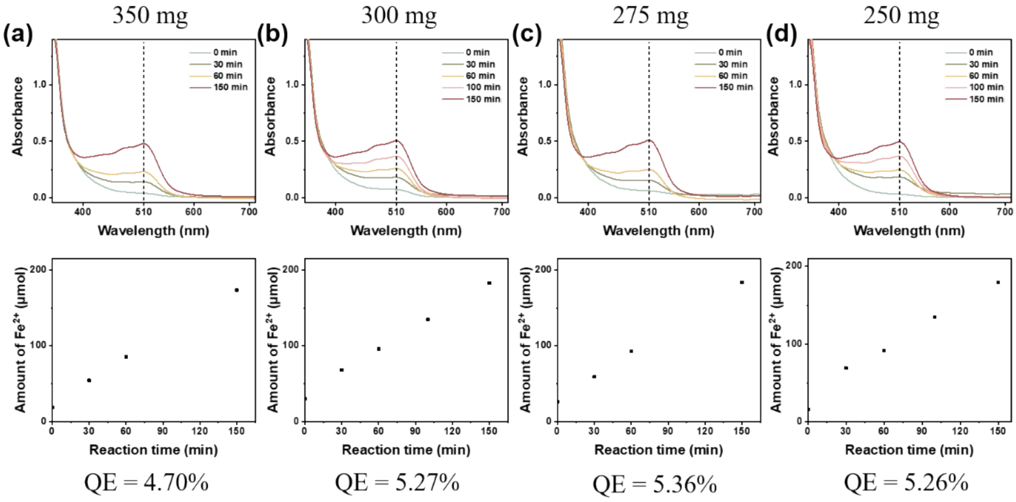

Fig. S4 Mass optimization and charge separation efficiency calculation for $BiVO_4$-7.0.

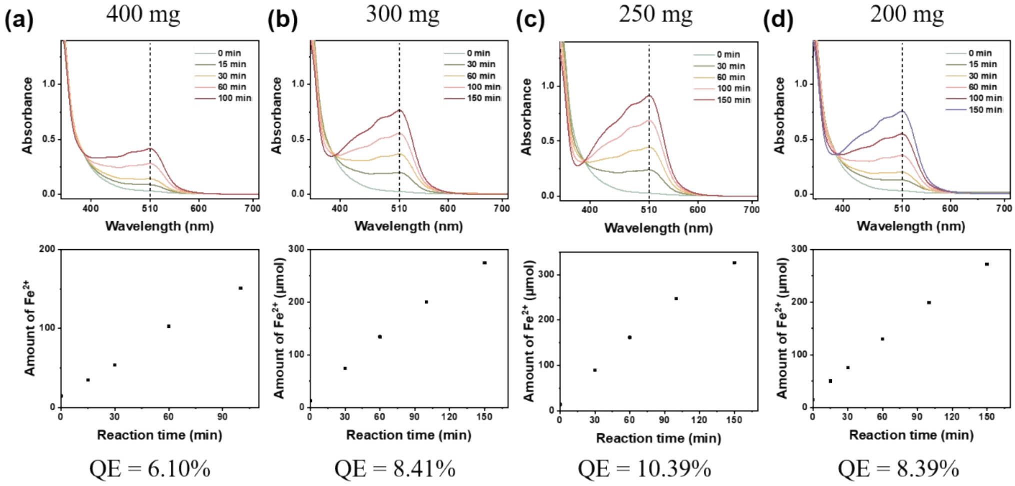

Fig. S5 Mass optimization and charge separation efficiency calculation for $BiVO_4$-3.8.

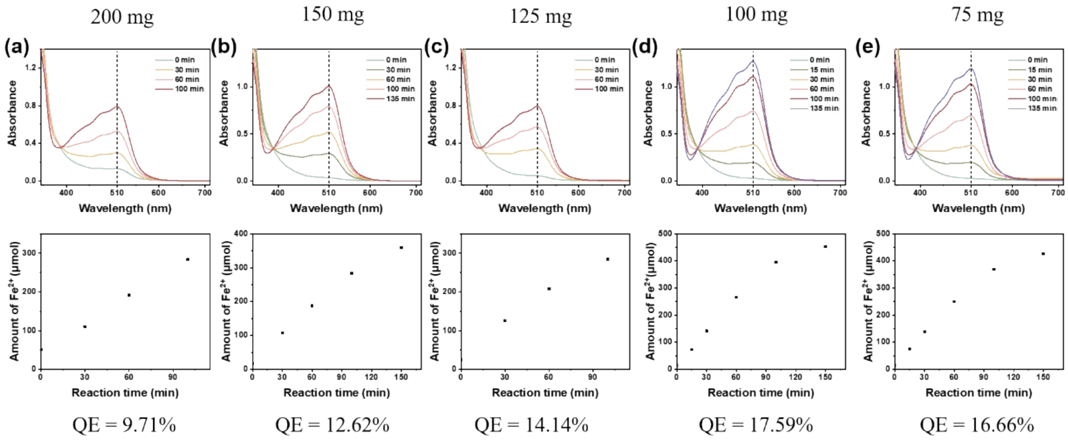

Fig. S6 Mass optimization and charge separation efficiency calculation for $BiVO_4$-1.0.

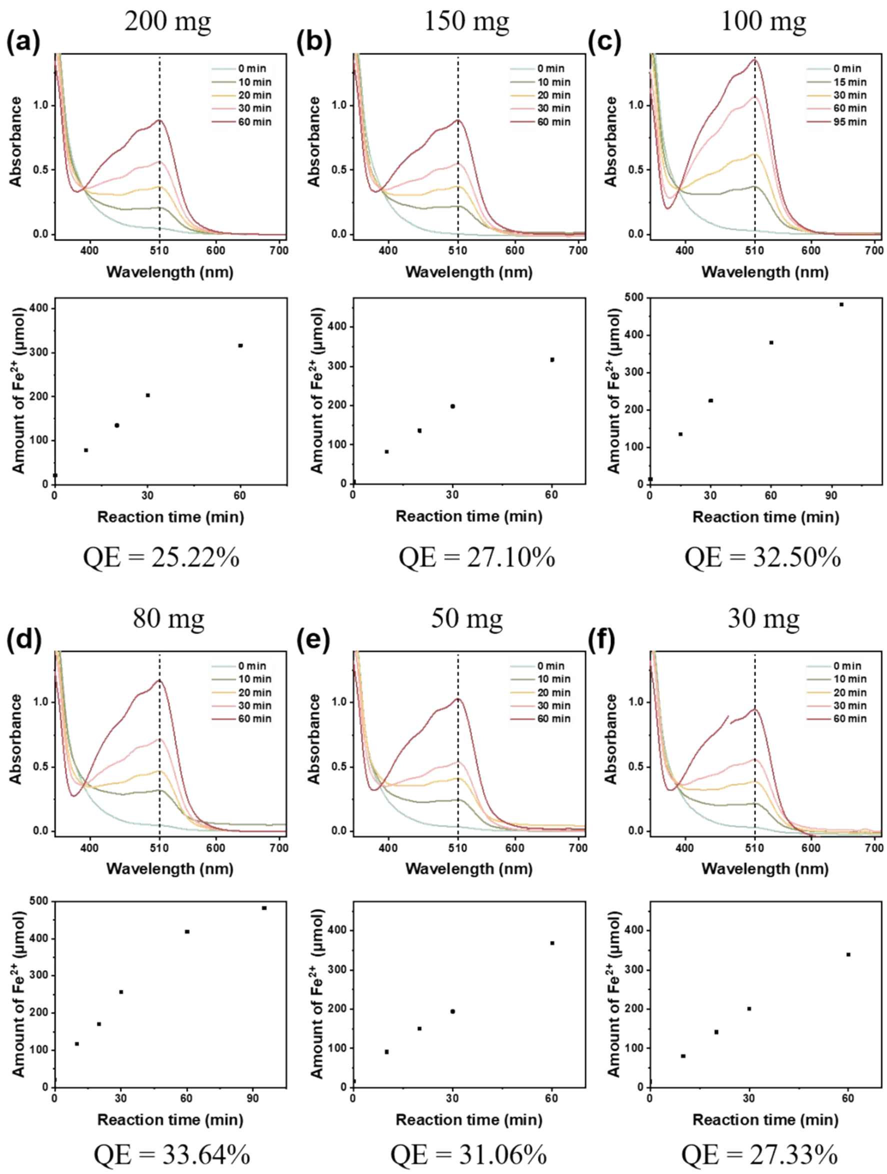

Fig. S7 Mass optimization and charge separation efficiency calculation for $BiVO_4$-0.1.

(a)

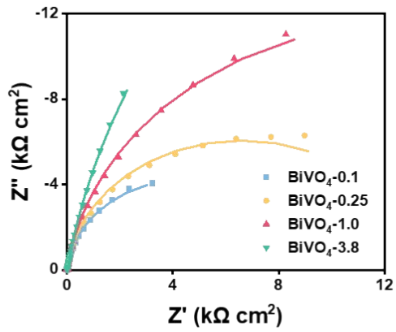

(b)

Samples	Rct (Ω)
$BiVO_4$-0.1	36321
$BiVO_4$-0.25	49939
$BiVO_4$-1.0	126930
$BiVO_4$-3.8	267140

Fig. S8 (a) Electrochemical impedance spectra (EIS) of octahedral $BiVO_4$ crystals with different sizes (solid line: fitted results) measured at 1.2 V versus RHE under light irradiation. (b) Equivalent circuit used for fitting the data; entries in the table are fitted from EIS results in (a).

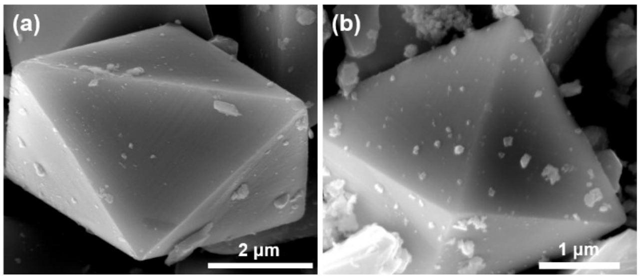

Fig. S9 The random deposition of Au nanoparticles on $BiVO_4$-5.5 by traditional impregnation method.

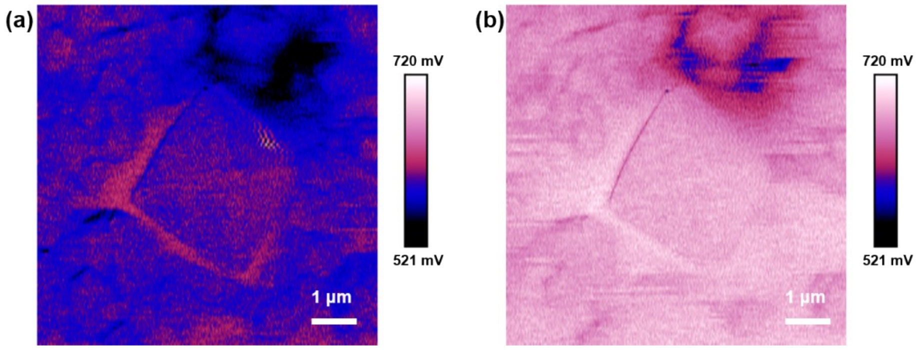

Fig. S10 KPFM images of octahedral $BiVO_4$ crystal under (a) dark and (b) light irradiation.

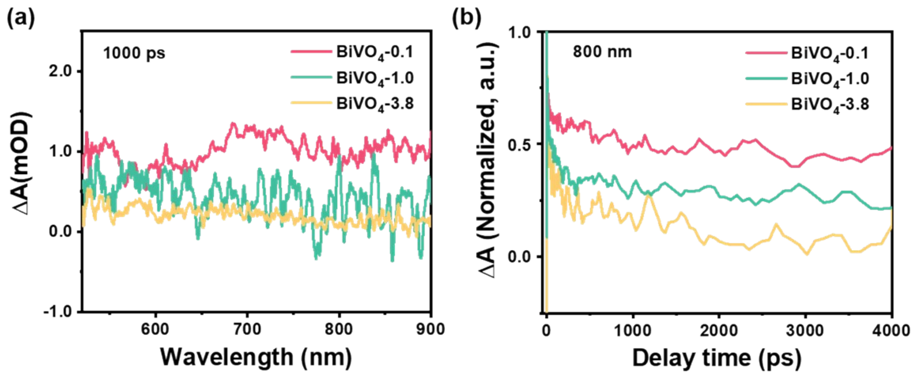

Fig. S11 (a) TA spectra of photogenerated holes for octahedral $BiVO_4$ crystals with varying sizes at 1000 ps delay following the excitation by a 400 nm pulse. (b) TA kinetics of photogenerated holes for octahedral $BiVO_4$ crystals with varying sizes probed at 800 nm.

Table S1. Charge separation efficiency over octahedral $BiVO_4$ with different sizes.

Sample	$BiVO_4$-7.0	$BiVO_4$-3.8	$BiVO_4$-1.0	$BiVO_4$-0.1
S_{BET} (m^2 g^{-1})	0.359	0.683	1.582	6.118
Optimized mass (mg)	275	250	100	80
Activity, r (μmol h^{-1})	76	150	254	471
AQE at 420 nm (%)	5.4	10.4	17.6	33.6
$\frac{r}{Mass \times S_{BET}}$ (μmol h^{-1} m^{-2})	706	878	1604	791
Bandgap (eV)	2.38	2.42	2.46	2.53

3. References

1. Y. Zhao, C. Ding, J. Zhu, W. Qin, X. Tao, F. Fan, R. Li and C. Li, *Angew. Chem. Int. Ed.*, 2020, **59**, 9653-9658.